Available online at www.sciencedirect.com
SCIENCE DIRECT®
Physica D 199 (2004) 185–193
PHYSICA D
www.elsevier.com/locate/physd

Characterization of spatiotemporal chaos in an inhomogeneous active medium

S. Bouzat[a], H.S. Wio[a,b,*], G.B. Mindlin[c]

[a] *Grupo de Física Estadística, Centro Atómico Bariloche (CNEA) and Instituto Balseiro (CNEA and UNC), 8400-San Carlos de Bariloche, Argentina*
[b] *Departament de Física, Universitat de les Illes Balears and IMEDEA (CSIC-UIB), E-07122 Palma de Mallorca, Spain*
[c] *Departamento de Física, FCEN, UBA, Ciudad Universitaria, Pab. I, CP 1428, Buenos Aires, Argentina*

Abstract

We study a reaction diffusion system of the activator–inhibitor type with inhomogeneous reaction terms showing spatiotemporal chaos. We analyze the topological properties of the unstable periodic orbits in the slow chaotic dynamics appearing, which can be embedded in three dimensions. We perform a bi-orthogonal decomposition analyzing the minimum number of modes necessary to find the same organization of unstable orbits.

PACS: 05.45.−a; 47.54.+r; 47.52.+j

Keywords: Active media; Spatiotemporal chaos; Bi-orthogonal decomposition

1. Introduction

Spatiotemporal chaos [1] has been extensively studied within the context of coupled maps, the complex Ginzburg–Landau equation, the Kuramoto–Shivashinsky equation and other related equations [2]. However, studies of spatiotemporal chaos in reaction–diffusion models closely connected to experimental systems are scarce. Here we analyze the characteristics of the chaotic dynamics recently found in a simple inhomogeneous reaction–diffusion system [3] of the type used to describe chemical reactions in gels [4] and patterns in coupled electrical circuits [5].

Among the main issues in the study of spatiotemporal chaos we can select those related to clarifying some aspects of the relation between pattern formation and chaos as well as the low-dimensional description of the chaotic behavior. The latter aspect, that is understanding that physically continuous systems with an infinity of degrees of freedom (spatially extended systems) usually show temporal behavior that can be well described by models with few degrees of freedom, is of extreme relevance. In this context there arise some questions. For instance, in low-dimensional dynamical systems, chaotic solutions coexist with unstable periodic orbits

* Corresponding author. Present address: Instituto de Física de Cantabria (UC-CSIC), Avda Los Castros s/n, 39005 Santander, Spain. Fax: +34 942 200 935.
E-mail address: wio@ifca.unican.es (H.S. Wio).

0167-2789/$ – see front matter © 2004 Elsevier B.V. All rights reserved.
doi:10.1016/j.physd.2004.08.013

which constitute the backbone of the strange attractor: could some orbits be extracted from the time series of our extended system? and, is the complex time evolution of the system of a dimensionality small enough to be understood in terms of simple stretching and folding mechanisms?

In order to investigate these questions within reaction–diffusion systems, we have analyzed the same simple, inhomogeneous, activator–inhibitor model discussed in Ref. [3]. It is worth remembering here that reaction–diffusion models of the activator–inhibitor type have provided a useful theoretical framework for describing pattern formation phenomena with applications ranging from physics to chemistry, biology and technology [6–8].

In Ref. [3] by introducing spatial dependence of the parameters of the activator–inhibitor equations, a system in which different parts of the media do not share the same reaction properties was modelled. The case considered corresponds to a finite one-dimensional oscillatory medium with an immersed bistable spot. In that system, in addition to stationary, Hopf-like and Turing-like patterns, quasiperiodic inhomogeneous oscillations and spatiotemporal chaos were also found. In Ref. [9], different generalizations of the system (bidimensional versions) have been studied. In the present paper we analyze the dynamics of the same one-dimensional system in the quasiperiodic and chaotic regions. More specifically, one of our main aims is to understand the topological properties of the chaotic dynamics. The model is given by the reaction–diffusion equations

$$\dot{u} = \partial_x^2 u - u^3 + u - v, \qquad \dot{v} = D_v \partial_x^2 v + u - \gamma v, \quad (1)$$

which describe a bistable medium for $\gamma > 1$ and an oscillatory one for $\gamma < 1$. In order to model the inhomogeneous situation of a bistable domain immersed in an oscillatory medium, a spatial dependence of this parameter is introduced setting $\gamma = \gamma(x) \equiv 0.9 + 5\exp(-10x^4)$ [10]. This leads to $\gamma \simeq 0.9 < 1$ for $|x| > 0.8$ (oscillatory medium) and $\gamma > 1$ for $|x| < 0.8$ (bistable medium). As was done in [3], we here consider a finite one-dimensional domain ($-L \leq x \leq L$) with non-flux boundary conditions in $\pm L$ and homogeneous initial conditions belonging to the homogeneous limit cycle that exists for the case $\gamma = 0.9$. This choice of the initial state corresponds to the description of an initially homogeneous oscillatory medium whose reaction properties are suddenly modified in a localized region.

In the central bistable region the fields converge rapidly to values close to those corresponding to one of the two natural states of the bistable medium ($u_\pm \simeq \pm 0.8$, $v_\pm \simeq \pm 0.14$) (chosen depending on the initial condition), and continue performing small amplitude oscillations around those values. Hence, there is a spontaneous symmetry breaking which is "inherited" from the properties of the (uncoupled) bistable medium. Note that the equations of the model are symmetric under the simultaneous changes $u \to -u$, $v \to -v$. The rest of the system evolves to different asymptotic behaviors depending on the parameters L and D_v as indicated in Fig. 1, and described in detail in [3].

All the numerical calculations have been done as follows. First, the system of partial differential equations was approximated by a system of coupled ordinary differential equations, obtained by a finite difference scheme. Then the resulting equations were solved by a Runge–Kutta method of order 2. Different space and time discretization schemes were employed in order to check the results.

The organization of the paper is the following. In the next section we show that, in the quasiperiodic and chaotic regimes, there are two dynamical time scales, a fast and a slow one. We show that it is possible to

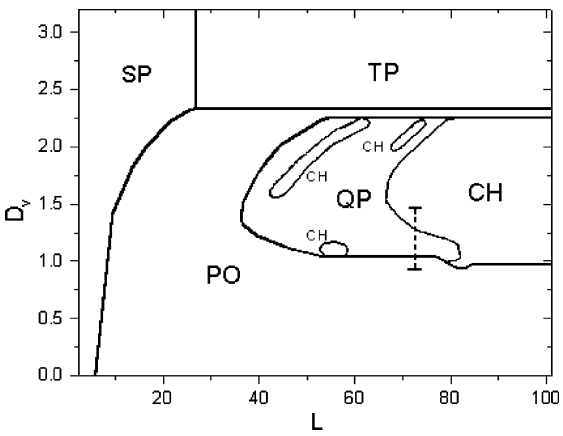

Fig. 1. Phase diagram indicating the different asymptotic regimes in the (L, D_v) plane: stationary patterns (SP), Turing patterns (TP), periodic inhomogeneous oscillations (PO), quasiperiodic oscillations (QP) and spatiotemporal chaos (CH). The vertical dotted segment indicates the region of main interest for this work.

find segments of the time series of the slow dynamics which approximate unstable periodic orbits and study the organization of the orbits. In Section 3, we present the bi-orthogonal decomposition of the spatiotemporal time series, and show that it is possible to capture the main features of the chaotic dynamics by considering a small number of modes. In Section 4 we present our conclusions.

2. Characterization of the slow chaotic dynamics: analysis of the unstable periodic orbits

In the non-stationary regions of the phase diagram shown in Fig. 1, the time evolution of the fields u and v is classified as periodic, quasiperiodic or chaotic [3]. Here, we analyze the transition from periodic oscillations to chaotic behavior along the line indicated with a vertical dotted segment in Fig. 1. We fix $L = 72$, for which the dynamics corresponds to inhomogeneous periodic oscillations for $D_v < 1$, quasiperiodic oscillations for $1 < D_v < 1.3$, and spatiotemporal chaos for $1.3 < D_v < 2$. (For $D_v > 2$ the quasiperiodic and periodic behaviors appear again and for $D_v > 2.3$ stationary Turing patterns arise.) To begin, we will mainly focus our attention on the chaotic region.

As a measure of chaoticity, in [3], the sensibility to initial conditions was computed. It is important to notice that the time series displayed a common feature: a fast oscillation of the field (at the natural frequency of the oscillatory medium), eventually modulated by a slow varying amplitude. It is the dynamics of this amplitude what we will analyze here. In order to study this slow dynamics we record the times t_n ($n = 1, 2, \ldots$) at which the u-field at $x = L$ reaches a local maximum as function of t (i.e., when $\partial_t u(x,t)|_{x=L} = 0$ and $\partial_t^2 u(x,t)|_{x=L} < 0$ holds simultaneously), and analyze the values of u for these times at different spatial positions. This is equivalent to taking a Poincare section, and is a way of averaging the fast time scales.

The difference $t_n - t_{n-1}$ is of the order of the natural period of the oscillatory medium ($\tau_0 = 14.6$), but slightly larger (in general, it fluctuates between τ_0 and 20) as the oscillations are slowed down by the presence of the bistable inhomogeneity. In the periodic region, $t_n - t_{n-1}$ converges to the period of the motion as $n \to \infty$.

Typical time series are shown in Fig. 2. In Fig. 2a and c, the time evolution of $u(L)$ is displayed for a parameter value at which the system behaves quasiperiodically (chaotically). The slow varying amplitude is shown in Fig. 2b and d, where we have plotted the values of the maxima of $u(L)$ as a function of t (i.e., $u(L)$ measured at times t_n).

In general, in low-dimensional dynamical systems, chaotic solutions coexist with unstable periodic orbits which constitute the backbone of the strange attractor. We will see that, in our system, it is possible to extract approximations of periodic unstable orbits from the time series of the mentioned slow dynamics, and that the analysis of the organization of these orbits shows that the chaotic dynamics is low-dimensional.

We begin by defining as *reconstructed periodic orbits* the segments of the time series which can be used as surrogates of the unstable periodic orbits of the system. These segments are chosen if they pass a close return test [11]. More precisely, if $y(i)$ represents the data, a close return is a segment of p points beginning at the ith position of the file, for which $y(i + k) \approx y(i + k + p)$ for $k = 1, 2, \ldots$. In this notation, p is called the period.

We have looked for unstable orbits at the whole time series of the slow dynamics of the u field (data taken at times t_n) at four different positions: $x_0 = 0$, $x_1 = 14$ (approximately one Turing wavelength away the bistable domain), $x \simeq x_2 = L/2 = 36$, and $x = L$.

In Fig. 3a and c we display a segment of periods 2 and 4 taken from a time series corresponding to data at $x = L$. An embedding of the data (a multivariate environment created using time delays) is shown in Fig. 3b and d. In Fig. 4a and b we show the embedding of two different reconstructed segments of periods 2 and 3, respectively, coming from data at $x = x_1$. It is worth mentioning that the unstable periodic orbits do not have properties corresponding to the inversion symmetry of Eq. (1) because of the symmetry breaking of the solutions and also because of the "stroboscopic" observation of the dynamics. In Fig. 4c, we show a more complex reconstructed periodic orbit coming also from data at $x = x_1$. Since we have no elements to conjecture that the chaotic dynamics can live in three dimensions, it could be argued that embedding the segments in a three-dimensional space might not be useful. Yet, if the reconstructed shows some kind of geometrical organization it would be a most valuable indication of the geometric process taking place in a

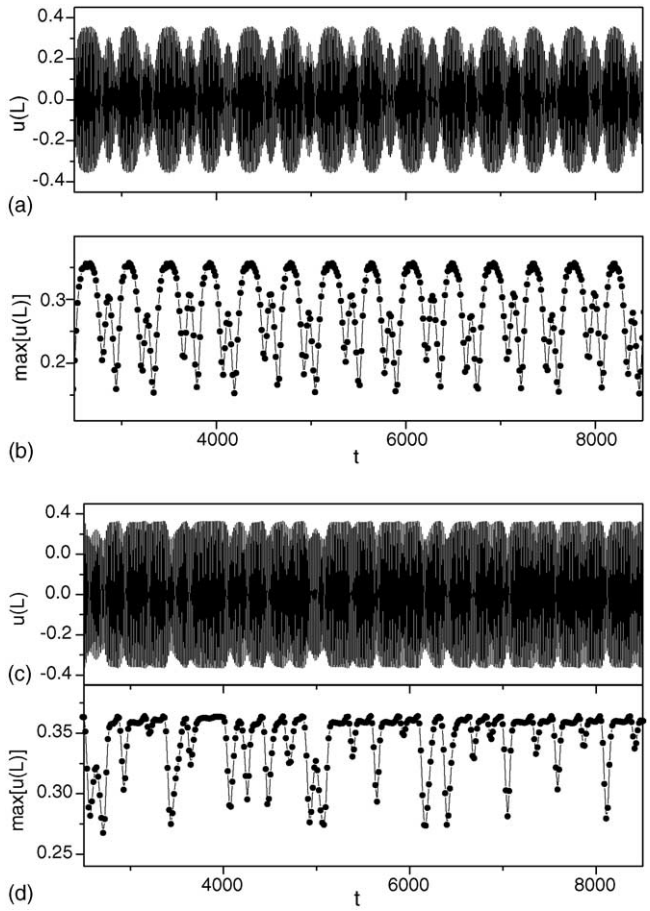

Fig. 2. (a) Evolution of $u(L)$ for $D_v = 1.1$ (quasiperiodic regime) in a time window in the asymptotic regime; (b) slow dynamics: plot of the maxima of $u(L)$ corresponding to the same time window; (c) and (d), ibidem figures (a) and (b) for $D_v = 1.4$ (chaotic regime).

small dimensional manifold within the available phase space.

It is possible to see that the orbits of Fig. 3b and d wind around each other as expected if they were related by a period doubling bifurcation. The topological organization of the orbits is quantitatively described in terms of their relative rotation rates and self-relative rotation rates. These numbers aim at describing the way in which the orbits wind around each other [12]. In order to do so, the curves are given an orientation, and in a two-dimensional projection, a record is made of which segments pass over which in the original embedded orbits. In terms of these indices, the relative rotation rates are computed as explained in [12]. For the period 2 orbit of Fig. 4a, the self-relative rotation rate is srrr $= -1/2, 0$, for the period 3 orbit of Fig. 4b, it is srrr $= (-1/3)^2, 0$, and the relative rotation rate between the orbits of periods 2 and 3 was found to be rrr $= -1/3$. Notice that this organization is compatible with a horseshoe mechanism [12], and that this mechanism includes the signature of period doubling.

A challenge exists in order to find a simple geometrical mechanism responsible for the creation of the orbit displayed in Fig. 4c. This orbit cannot be placed in a horseshoe template. Yet, recently, a classification of templates was proposed for covering the Smale horseshoe [13]. We have observed that the orbit of Fig. 4c can be placed in one of such geometric objects, which is one of the four inequivalent four-branched *double covers* with rotation symmetry of the Smale. More

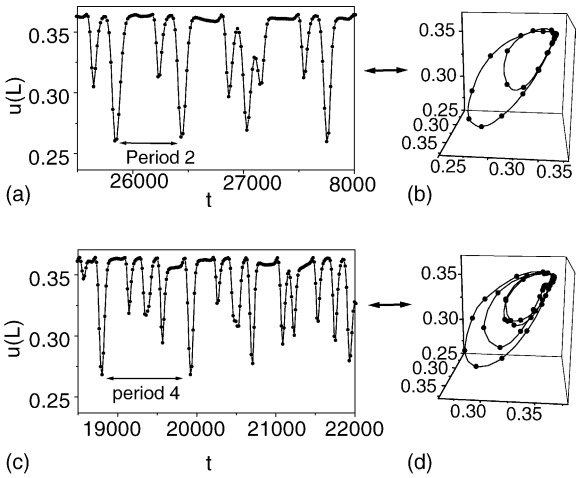

Fig. 3. (a) Slow dynamics: values of the field $u(L)$ at times t_n for a time window in which a segment corresponding to a period 2 orbit appears. Note that the segment is repeated almost twice. (b) Period 2 orbit corresponding to the segment indicated in (a) obtained from an embedding in three dimensions using time delays (the axis correspond to the data taken at t_n, t_{n+1} and t_{n+2}). (c) Idem (a) for a period 4 orbit. (d) Embedding of the segment of (c). All the data correspond to a simulation done for $D_v = 1.4$.

specifically, the one identified with topological indices $(n_0, n_1) = (1, 0)$ [13]. This template can also hold any orbit of the Smale horseshoe template.

However, it cannot be expected that such template correctly describes the whole dynamics of the slow varying amplitude. This is because it is not possible that a rotation symmetry appear when using a delay embedding. Hence, the embedded attractor must have a different symmetry or not symmetry at all, and it is expected that other unstable periodic orbits exist (different to the ones we have found and with no rotation symmetry).

Note that, when observing the u-field at times t_n, it is found that the scales over which it varies are quite different at the four studied positions (x_0, x_1, x_2 and x_L): at $x = L$, $u(t_n)$ oscillates between 0.2 and 0.35 (since we are watching only the times at which $u(L, t)$ is maximum); at $x = x_1$ and $x = x_2$, $u(t_n)$ take values in a more or less symmetric way between ± 0.35 (in the whole range of the free limit cycle); at $x = x_0$ (in the bistable domain) the oscillations are of much smaller amplitude (typically two orders of magnitude), and are not centered at zero. We remark that, in spite of these differences in the metrical properties of the dynamics at the several positions, the organization of the unstable periodic orbits that we have found is the same everywhere. (In the four positions we find the same kind of orbits, including the one of Fig. 4c.) However, there are some differences in the frequency of occurrence of the orbits: note that, we have orbits with the "small curl" upward (as in Fig. 3b) or downward (as in Fig. 4a). The same two possibilities appear for orbits of periods 3 and 4. For the cases of the signal taken at x_0, x_1 and x_2, the orbits of periods 2 and 3 occur preferably with the small curl downward, while, for $x = L$ they occur (almost always) with the small curl upward. This is found independently of whether the fields in the bistable domain converge to negative or positive values.

The observation that the organization of unstable periodic orbits is more complex, but some how related to the one of the Smale horseshoe, gives a hint of what kind of periodic orbits can eventually be found as parameters are changed. For example, it suggest that a period doubling sequence may occur in the transition from the periodic regime to the chaotic regime. With this in mind, we revisited in detail the transition zone in the phase diagram of the system going from the periodic region to the chaotic one along the segment indicated in Fig. 1. A period doubling of the slow dynamics can be clearly identified, as can be seen in Fig. 5.

The analysis made of the slow dynamics of our extended system showed that the high dimension of the phase space is not fully explored. On the contrary, an important collapse of dimensionality takes place. In the next section we investigate the minimum number of spatial (linear) modes approximating the spatiotemporal dynamics that are required in order to recover the topological organization of unstable periodic orbits observed in the slow dynamics.

3. Bi-orthogonal decomposition

It is not easy to know a priori which is the number of spatial modes which are activated as the dynamics becomes non-trivial. In our problem, we only know that at least three modes should be active in order to account for the complex behavior described in the previous section. A method exists to unveil the active structures in a spatiotemporal problem: the bi-orthogonal decomposition (BOD) [14,15]. This is the most efficient linear decomposition scheme, in the sense that there is no other linear decomposition able to capture, with a smaller

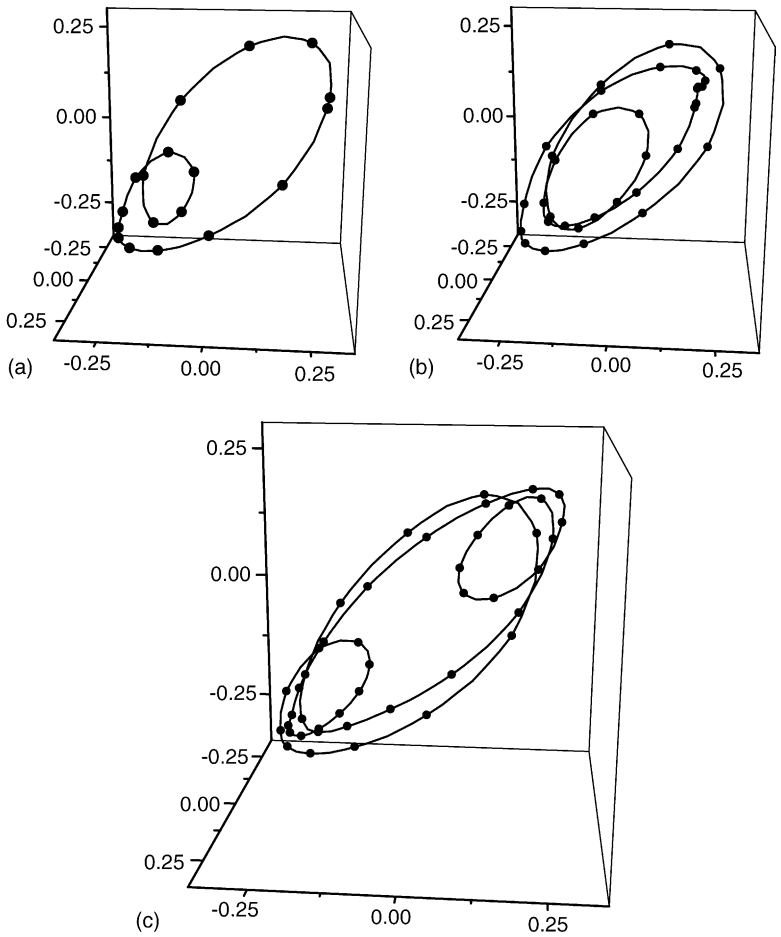

Fig. 4. Periodic orbits reconstructed from data taken at $x = x_1 \equiv 14$ at the times t_n using an embedding of time delays with axis t_n, t_{n+1}, t_{n+2}: (a) period 2 orbit; (b) period 3 orbit; (c) complex periodic orbit.

number of modes, the same degree of approximation. In our system, the BOD for the spatiotemporal signal $(u(x,t), v(x,t))$ is given by

$$(u(x,t), v(x,t)) = \sum_{k=1}^{\infty} \alpha_k \psi_k(t) \vec{\phi}_k(x), \tag{2}$$

where the α_k^2 (with $\alpha_1 > \alpha_2 > \cdots > 0$) are the eigenvalues of the temporally averaged two point correlation matrix [14], the $\vec{\phi}_k(x) = (\phi_{uk}(x), \phi_{vk}(x))$ are the corresponding eigenfunctions (called topos), and the $\psi_k(t)$ (called chronos) are given by

$$\psi_k(t) = \frac{1}{\alpha_k} \int_0^L (u(x,t)\phi_u(x) + v(x,t)\phi_v(x))\,\mathrm{d}x. \tag{3}$$

We have observed that, for system (1), the main differences in the BOD corresponding to the three dynamical regimes appear in the chronos and that the spatial modes are similar in all the three cases. However, we have neither studied in detail the BOD along the transition to chaos nor analyzed the question of modes' competition. Our analysis was mainly focused on finding the number of modes that are necessary to recover the topological organization of unstable orbits for the chaotic situation presented in the previous section.

In Fig. 6a we show the eigenvalues of the BOD computed for three different points along the transition line indicated in Fig. 1: a periodic case, a quasiperiodic case and the chaotic situation studied in the previous section. In Fig. 6b we show the first four topos for the

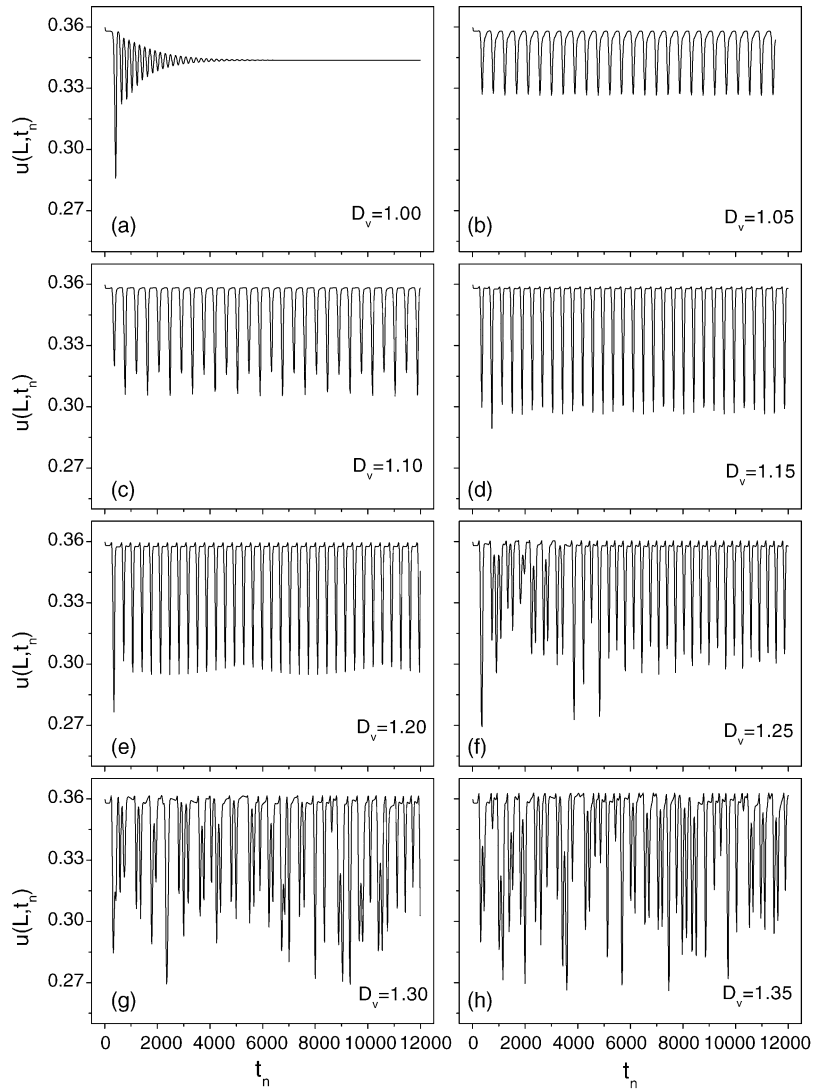

Fig. 5. Slow dynamics time series showing a period doubling sequence. Plots of $u(x = L)$ at times t_n for different values of D_v (indicated in the figure) following the transition from periodic regime to quasiperiodic and chaotic. (a) The periodic region where a fixed point occurs in the slow dynamics. (b)–(e) The quasiperiodic region, orbits of periods 1, 2, 4 and 16 are respectively observed in the slow dynamics. (f) A quasiperiodic regime showing a chaotic-like transient followed by high-period orbit (not identifiable in the figure). (g) and (h) The chaotic regime. Al calculations are for $L = 72$.

chaotic case. No significant differences are observed in the spatial modes corresponding to the three regimes. We have observed that, in all the three regimes, the ith mode has $i - 1$ spatial nodes (i.e., the spatial points where $u(x) = 0$), see Fig. 6b. Also, in all the three cases, the second mode is quasi-stationary and it mainly contributes to the formation of the fields' profiles in the (quasi-stationary) bistable region. (Note that the topo 2 in Fig. 6b contributes only around the bistable region ($x \sim 0$).)

In the case of periodic motion, in order to reconstruct the trivial topology of a single periodic orbit, only the first mode is necessary (which gives a quasi-homogeneous periodic oscillation). Moreover, in this

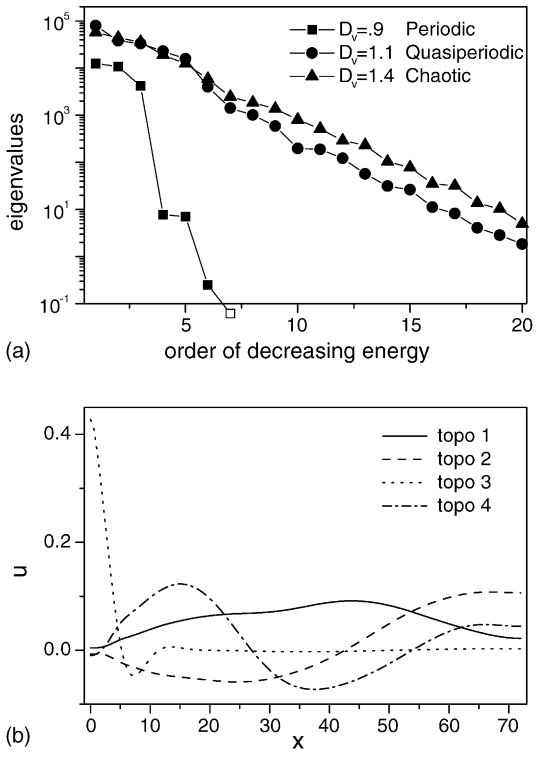

Fig. 6. Bi-orthogonal decomposition: (a) eigenvalues for three different values of D_v corresponding to chaotic, quasiperiodic and periodic regimes; (b) u-field components of the four principal topos (corresponding to the four larger eigenvalues) for the chaotic case with $D_v = 1.4$.

region, we have observed that the whole spatiotemporal dynamics (i.e., the periodic wave propagation phenomenon) can be highly accurately described by considering an expansion with only three modes (2), as it is suggested by Fig. 6a. Regarding the description of quasiperiodic and chaotic motion, it requires a higher number of modes, as can be inferred from Fig. 6a. In these regimes all the chronos seems to be non-periodic (excepting the second, which is constant up to a good approximation).

Finally, for the chaotic case analyzed in the previous section, we have reconstructed the dynamics of the system using different numbers of modes. The main result of our analysis is that the minimum number of modes required to recover the topological organization of orbits is five. This means that using five modes (and not four) we were able to recover the orbits presented in the previous section. There seems to be neither something special in this number, nor a way of having predicted it a priori. However, it is important to point out that the extended system under study can in principle display an infinite dimensional dynamics, and yet, it dynamically collapses to a five-dimensional system which describe the dynamics of the amplitudes of the linear modes. Furthermore, it is remarkable that the fact that five modes are active does not imply that the dimensionality of the observed strange attractor is larger than four. On the contrary, the topological organization of the approximated unstable periodic orbits clearly suggest a lower dimensionality.

4. Conclusions

In this work we studied the spatiotemporal solutions of a reaction–diffusion system of the activator–inhibitor type. Despite the infinite number of possible degrees of freedom, we have found that the complex dynamics that emerges can be described in terms of a small number of modes. The activated modes are coherent structures which were computed from the simulations of this extended problem. By separating the dynamics over two time scales, we observed that the origin of the chaoticity lies on the behavior of the slow time scale dynamics. The study of these time series showed not only that the system behaves as a small dimensional dynamical system, but also suggest that this dynamics may be understood in terms of simple geometrical process related to the Smale horseshoe. In fact, a branched manifold recently described in the literature can hold all the approximated unstable orbits that we were able to reconstruct. However, symmetry reasons indicate that the true mechanism should not be exactly the one corresponding to that template. The description of the dynamics in terms of a simple geometric structure not only highlights the collapse of dimensionality, but it also allowed us to predict the existence of specific solutions for unexplored regions of parameter space, such as the reported period doubling sequence.

Acknowledgments

To Verónica Grunfeld for reading the manuscript. Partial support from ANPCyT and UBACyT, Argen-

tine agencies, is also acknowledged. SB and GB thanks for the kind hospitality extended to them during their stays at the DF (UBA) and IB-CAB, respectively. HSW thanks the MECyD, Spain, for an award within the *Sabbatical Program for Visiting Professors*, and to the Universitat de les Illes Balears for the kind hospitality extended to him.

References

[1] M.C. Cross, P.C. Hohenberg, Rev. Mod. Phys. 65 (1993) 851.
[2] K. Kaneko, Physica D 34 (1989) 1;
P.C. Hohenberg, B.I. Shraiman, Physica D 37 (1989) 109;
B.I. Shraiman, et al., Physica D 57 (1992) 241;
A. De Wit, G. Dewel, P. Borckmans, Phys Rev. E 48 (1993) R4191;
R. Montagne, et al., Phys Rev. E 56 (1997) 151 (see also Sect. VII of Ref. [1]).
[3] S. Bouzat, H.S. Wio, Phys Lett. A 268 (2000) 323.
[4] J.J. Tyson, P.C. Fife, J. Chem. Phys. 73 (5) (1980) 2224;
S. Kádár, J. Wang, K. Showalter, Nature 391 (1998) 770;
A. Horváth, M. Dolnik, A.P. Muñuzuri, A. Zhabotinsky, I. Epstein, Phys. Rev. Lett. 83 (1999) 2950.
[5] G. Heidemann, M. Bode, H.G. Purwins, Phys Lett. A 177 (1993) 225.
[6] J.D. Murray, Mathematical Biology, Springer-Verlag, 1985.
[7] A.S. Mikhailov, Foundations of Synergetics I, Springer-Verlag, 1990.
[8] D. Walgraef, Spatio-Temporal Pattern Formation, Springer-Verlag, New York, 1997;
E. Meron, Phys. Rep. 218 (1992) 1.
[9] S. Bouzat, H.S. Wio, Phys. Rev. E 63 (2001) 056213 (10 pages).
[10] The exact shape of this function is unimportant, as was discussed in [3] and [9].
[11] G.B. Mindlin, R. Gilmore, Physica D 58 (1992) 229.
[12] R. Gilmore, Rev. Mod. Phys. 70 (4) (1998).
[13] C. Letellier, R. Gilmore, Phys. Rev. E 63 (2000) 016206.
[14] N. Aubry, R. Guyonnet, R. Lima, J. Stat. Phys. 64 (1991) 683.
[15] P. Holmes, J.L. Lumely, G. Berkooz, Turbulence, Coherent Structures Dynamical Systems and Symmetry, Cambridge University Press, 1997.